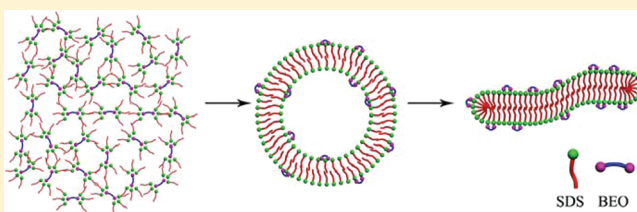


# Aggregate Transitions in Aqueous Solutions of Sodium Dodecylsulfate with a “Gemini-Type” Organic Salt

Defeng Yu,<sup>†</sup> Maozhang Tian,<sup>†</sup> Yaxun Fan,<sup>†</sup> Gang Ji,<sup>‡</sup> and Yilin Wang\*,<sup>†</sup>

<sup>†</sup>Key Laboratory of Colloid and Interface Science, Beijing National Laboratory for Molecular Sciences (BNLMS), Institute of Chemistry and <sup>‡</sup>Center for Biological Electron Microscopy, Institute of Biophysics, Chinese Academy of Sciences, Beijing 100190, People's Republic of China

**ABSTRACT:** Effects of a “gemini-type” organic salt 1,2-bis(2-benzylammoniummethoxy) ethane dichloride (BEO) on the aggregation behavior of sodium dodecylsulfate (SDS) have been investigated by turbidity, surface tension, isothermal titration microcalorimetry, dynamic light scattering, cryogenic transmission electron microscopy, <sup>1</sup>H NMR spectroscopy, and differential scanning microcalorimetry. The aggregation behavior of the SDS/BEO mixed aqueous solution shows strong concentration and ratio dependence. For the SDS/BEO solution with a molar ratio of 5:1, large loose irregular aggregates, vesicles, and long thread-like micelles are formed in succession with the increase of the total SDS and BEO concentration. Because BEO has two positive charges, the SDS/BEO solution may consist of the (SDS)<sub>2</sub>–BEO gemini-type complex, the SDS–BEO complex and extra SDS. The aggregation ability and surface activity of the SDS/BEO mixture exhibit the characteristics of gemini-type surfactants. Along with the results of DSC and <sup>1</sup>H NMR, the (SDS)<sub>2</sub>–BEO gemini-type structure is confirmed to exist in the system. This work provides an approach to construct the surfactant systems with the characteristics of gemini surfactants through intermolecular interaction between a two-charged organic salt and oppositely charged single-chain surfactants.



## INTRODUCTION

Surfactant molecules can self-assemble into highly organized aggregates with various kinds of morphologies in aqueous solutions, including spherical micelles, worm-like or thread-like micelles, vesicles, bilayers, nanotubes, and so on.<sup>1–3</sup> All of these aggregates are related to the wide applications of surfactants. Researchers have made great efforts to develop highly efficient surfactants with various molecular structures. Gemini surfactants are one kind of the highly efficient surfactants. Compared with conventional single-chain surfactants, gemini surfactants show many unique properties, such as high surface activity, low critical micelle concentrations (CMC), unusual aggregate morphologies, and so on.<sup>4–6</sup> However, complicated synthesis procedures limit the development and industrial applications of the novel surfactants. If gemini-type surfactants can be constructed through intermolecular interaction between single-chain surfactants and a gemini-type connection molecule, it will open a new facile approach to obtain highly efficient surfactants. An organic salt with two connecting points to ionic surfactants should be a possible choice as a gemini-type connection molecule.

A kind of organic salt can be constructed by aromatic groups and several charged substituents. Recently, Nalluri and Ravoo<sup>7</sup> applied the photoisomerization of a bifunctional noncovalent linker molecule to induce and reverse molecular recognition and adhesion of vesicles. The linker molecule was constructed by two functional azobenzenes covalently bound with a hydrophilic spacer. Being inspired by the linker molecule, we realized that gemini-type surfactants could be constructed by a

“gemini-type” organic salt, in which two charged substituents and two benzene rings are covalently linked with a spacer. If the two charged substituents with two benzene rings bind with two oppositely charged surfactant molecules through strong electrostatic interaction assisted by hydrophobic interaction and  $\pi$ – $\pi$  interaction, the resultant complexes may show similar properties to gemini surfactants. Moreover, the aggregates of the complexes may be linked with each others by the “gemini-type” organic salt, which may enrich the aggregate structures.

In this paper, the aggregation behavior of a “gemini-type” organic salt 1,2-bis(2-benzylammoniummethoxy) ethane dichloride (BEO) (Figure 1) with sodium dodecylsulfate (SDS) has

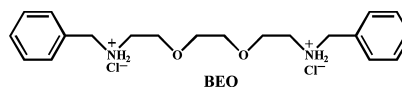


Figure 1. Chemical structure of “gemini-type” organic salt BEO.

been investigated. The aggregation behavior of the SDS/BEO mixed system shows strong concentration dependence and ratio dependence. When the SDS/BEO ratio is close to the neutralization point, precipitation takes place. While the SDS/BEO ratio is away from the neutralization point, the SDS/BEO mixtures exhibit special aggregate transitions. The SDS/BEO

Received: November 28, 2011

Revised: May 21, 2012

Published: May 21, 2012

solution is a mixture of the  $(SDS)_2$ -BEO gemini-type complex, the SDS–BEO complex, and extra SDS. The aggregation ability and surface activity of the mixtures are quite similar to those of the similar gemini surfactants. All of the results indicate that the gemini-type complexes can be constructed through intermolecular electrostatic binding between the two-charged “gemini-type” organic salt and oppositely charged SDS, assisted by the hydrophobic interaction between the hydrocarbon chains of SDS and the  $\pi$ – $\pi$  interaction between the benzene rings of BEO.

## ■ EXPERIMENTAL SECTION

**Materials.** SDS (BRL, 99.5%) was used as received. 1,2-Bis(2-benzylaminoethoxy) ethane (GC, >97%) was purchased from TCI (Shanghai) Development Co., Ltd. 1,2-Bis(2-benzylaminoethoxy) ethane was suspended in ethanol and neutralized by adding hydrochloric acid with at least twice the molar volume. Then, the product was cleaned with ethanol several times and freeze-dried. The purity of the obtained BEO was characterized by elemental analysis. Anal. Calcd for  $C_{20}H_{30}N_2O_2Cl_2$  (BEO): C, 59.85; H, 7.48; N, 6.98; Cl, 17.71. Found: C, 59.99; H, 7.52; N, 6.82; Cl, 17.55. Milli-Q water (18  $M\Omega \cdot cm^{-1}$ ) was used throughout.

**UV–Vis Experiments.** The absorption spectra were recorded in quartz cuvettes (path length 1 cm) by a SHIMADZU UV 1601PC spectrometer. The absorbance at 400 nm was chosen as the turbidity. All of the measurements were conducted at  $25 \pm 2^\circ\text{C}$ .

**Surface Tension Measurement.** Surface tension measurements were carried out by the drop volume method<sup>8</sup> at  $25.00 \pm 0.05^\circ\text{C}$ .

**Isothermal Titration Microcalorimetry (ITC).** Calorimetric measurements were conducted using a TAM 2277-201 microcalorimetric system (Thermometric AB, Järfälla, Sweden) with a stainless steel sample cell of 1 mL at  $25.00 \pm 0.01^\circ\text{C}$ . The cell was initially loaded with 0.8 mL of pure water. The concentrated SDS/BEO mixed solution was injected into the sample cell via a 500  $\mu\text{L}$  Hamilton syringe controlled by a 612 Thermometric Lund pump. A series of injections were made until the desired range of concentrations had been covered. The system was stirred at 50 rpm with a gold propeller. The observed enthalpy ( $\Delta H_{\text{obs}}$ ) was obtained by integration over the peak for each injection in the plot of heat flow  $P$  against time  $t$ .

**Dynamic Light Scattering (DLS).** Measurements were carried out at  $25.0 \pm 0.5^\circ\text{C}$  by an LLS spectrometer (ALV/SP-125) with a multi- $\tau$  digital time correlator (ALV-5000). A solid-state He–Ne laser (output power of 22 mW at  $\lambda = 632.8\text{ nm}$ ) was used as a light source, and the measurements were conducted at a scattering angle of  $90^\circ$ . The freshly prepared samples were injected into a 7 mL glass bottle through a 0.45  $\mu\text{m}$  filter prior to measurements. The turbid solution was not filtered because large aggregates could be filtered in the process. The correlation function of the scattering data was analyzed via the CONTIN method to obtain the distribution of diffusion coefficients ( $D$ ) of the solutes, and then, the apparent equivalent hydrodynamic radius ( $R_h$ ) was determined by using the Stokes–Einstein equation  $R_h = kT/6\pi\eta D$ , where  $k$  is the Boltzmann constant,  $T$  is the absolute temperature, and  $\eta$  is the solvent viscosity.

**Cryogenic Transmission Electron Microscopy (Cryo-TEM).** The SDS/BEO mixed solutions were embedded in a thin layer of vitreous ice on freshly carbon-coated holey TEM

grids by blotting the grids with filter paper. Then, the grids were plunged into liquid ethane cooled by liquid nitrogen. Frozen hydrated specimens were imaged by using an FEI Tecnai 20 electron microscope (LaB6) operated at 200 kV with the low-dose mode (about 2000 e/ $\text{nm}^2$ ) and nominal magnification of 50 000. For each specimen area, the defocus was set to 1–2  $\mu\text{m}$ . Images were recorded on Kodak SO163 films and then digitized by a Nikon 9000 with the scanning step of 2000 dpi corresponding to 2.54  $\text{\AA}/\text{pixel}$ .<sup>9</sup>

**$^1\text{H}$  NMR.**  $^1\text{H}$  NMR spectra were recorded by using a Bruker AV400 FT-NMR spectrometer operating at 400.1 MHz at  $23 \pm 2^\circ\text{C}$ . Deuterium oxide (99.9%) was from CIL (Cambridge Isotope Laboratories) and used to prepare the SDS/BEO solutions at different concentrations. About 1 mL of solution was transferred to a 5 mm NMR tube for each measurement. Chemical shifts were given as the  $\delta$  (ppm) scale. The center of the HDO signal (4.790 ppm) was used as the reference in the  $\text{D}_2\text{O}$  solutions. The digital resolution of the NMR spectra was 0.04 Hz/data point. The signal assignments of BEO were determined by the 2D NOESY method.

**Differential Scanning Calorimetry (DSC).** The DSC thermograms of the SDS/BEO mixed solutions were obtained using a VP-DSC microcalorimetric system (MicroCal, U.S.A.). The surfactant solutions were degassed for 15 min, while pure water was degassed for 5 min. The mixed solution was transferred into a Tantaloy 61 alloy sample cell of 500  $\mu\text{L}$ , and the final weight was taken. The sample cell containing the mixed solution and the reference cell with water were cooled down to  $-10.0^\circ\text{C}$ . The DSC thermograms were recorded at a heating rate of 90  $^\circ\text{C}/\text{h}$  through the instrument software.

## ■ RESULTS AND DISCUSSION

Electrostatic binding between dicationic “gemini-type” organic salt BEO and anionic single-chain surfactant SDS may cause phase separation in the mixed aqueous solutions. Therefore, first, the phase separation at different SDS/BEO molar ratios and a fixed SDS concentration of 40 mM in aqueous solution were examined, and the results are shown in Table 1. The SDS/

**Table 1. Solution State of the SDS/BEO Solution at 40 mM SDS and Different SDS/BEO Molar Ratios**

SDS/BEO	20:1	10:1	5:1	4:1	3:1	2.5:1	2:1
solution state	clear (for at least 3 months)		precipitate (after 1 week)		precipitate (at once)		

BEO mixed solutions were clear even at the SDS/BEO molar ratio of 3:1. Only when the charge ratio of SDS/BEO reached  $\sim 1:1$ , that is, the SDS/BEO molar ratio of 2.5:1 or 2:1, the mixed solution became turbid, where precipitation took place.

On the basis of the above observation of the phase separation, the following investigations were focused on the clear solutions with higher SDS/BEO molar ratios, that is, 5:1, 10:1, and 20:1.

Interestingly, it was found that the mixed solutions became turbid (not precipitation) at the low total concentration of SDS and BEO while diluting the clear SDS/BEO solutions at the SDS/BEO molar ratios of 5:1, 10:1, and 20:1. The turbidity values of the SDS/BEO mixed solutions at different molar ratios were monitored by UV–vis absorbance at 400 nm and are expressed against the SDS concentration in Figure 2a. The SDS/BEO mixed solutions are clear, and the turbidity is zero below 0.4 mM SDS. As the SDS concentration gradually

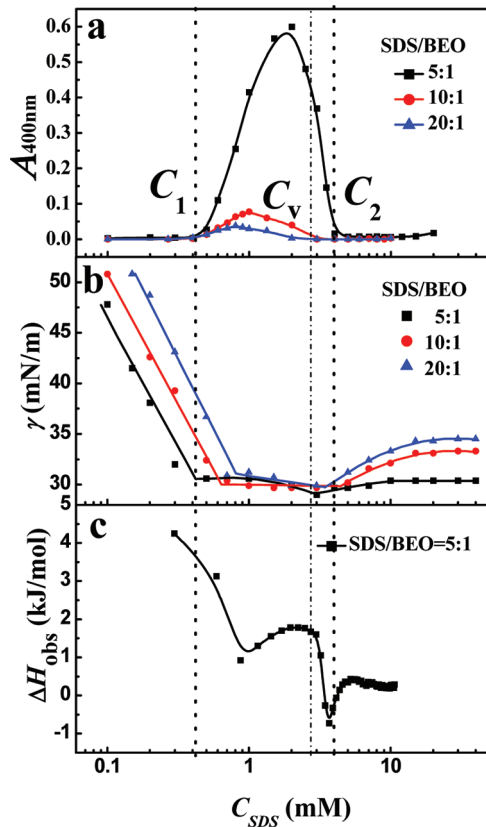


**Figure 2.** (a) Turbidity at 400 nm ( $A_{400\text{ nm}}$ ), (b) surface tension ( $\gamma$ ), and (c) observed enthalpy changes ( $\Delta H_{\text{obs}}$ ) versus the logarithm of the SDS concentration ( $C_{SDS}$ ).

increases, the turbidity suddenly arises, then reaches a maximum between 2 and 3 mM SDS, and finally decreases to 0 again at about 4 mM SDS. The SDS concentrations corresponding to the starting point of the turbidity increase and the ending point of the turbidity decrease are designated as  $C_1$  and  $C_2$ , respectively. Especially, the maximum of the turbidity between  $C_1$  and  $C_2$  greatly increases with the decrease of the SDS/BEO molar ratio. According to the structures of SDS and BEO, SDS and BEO may form the  $(\text{SDS})_2$ -BEO gemini-type complexes and the SDS-BEO complexes in the solution. Thus, the SDS/BEO solution consists of the  $(\text{SDS})_2$ -BEO gemini-type complexes, the SDS-BEO complexes, and extra free SDS molecules. Because normally gemini surfactants exhibit much stronger aggregation ability than single-chain surfactants, the larger turbidity at a lower SDS/BEO molar ratio between  $C_1$  and  $C_2$  implies that the relative content of the  $(\text{SDS})_2$ -BEO gemini-type structure should be higher when the initial mixing molar ratio of SDS to BEO is lower. Correspondingly, free SDS molecules should be less at a lower SDS/BEO mixing molar ratio than that at the higher one. Obviously, the results above suggest that the  $(\text{SDS})_2$ -BEO gemini-type structure significantly strengthens the aggregation ability of the mixture and results in larger aggregates.

In order to confirm the existence of the  $(\text{SDS})_2$ -BEO gemini-type structure, the surface tension values of the mixed solutions at different SDS/BEO molar ratios were studied, and the surface tension curves are shown in Figure 2b. All three surface tension curves are very similar. Upon increasing the SDS concentration, the surface tension linearly drops first, then slowly decreases or becomes constant beyond the first break

point ( $C_1$ ), starts to increase at the second break point ( $C_2$ ), and finally becomes constant again. The first break points  $C_1$  are about 0.4, 0.7, and 0.8 mM for the SDS/BEO molar ratios of 5:1, 10:1, and 20:1, respectively. These values are far below the CMC of pure SDS (8.7 mM)<sup>10</sup> in water and can be considered as the critical aggregation concentration of the mixtures of SDS with BEO. For the three different SDS/BEO molar ratios, the surface tension values at  $C_1$  are in the range of 29–31 mN/m, which are much lower than that of the pure SDS solution at its CMC (~38 mN/m).<sup>10</sup> Both the lower  $C_1$  values and lower surface tension indicate that the characteristics of the mixed system resemble the nearest related gemini surfactant. In addition, beyond  $C_2$ , the surface tension value is lower at the lower SDS/BEO molar ratio. Given that normally gemini surfactants are much more surface-active, this supports that the mixture contains the  $(\text{SDS})_2$ -BEO gemini-type structure and that the relative content of the gemini-type structure is higher at the lower SDS/BEO molar ratio. The gemini-type structure enhances the close packing of the SDS molecules at the air–water interface. Very recently, Jiang et al.<sup>11</sup> reported the properties and phase boundaries of the aqueous mixtures of dodecyltrimethylammonium bromide ( $\text{C}_{12}\text{TAB}$ ) with sodium oligoarene sulphonates ( $\text{POS}_n$ ). The behavior of POS2 and POS3 is reasonably consistent with mixed micelles of  $\text{C}_{12}\text{TAB}$  and  $\text{POS}_n$ -( $\text{C}_{12}\text{TA}$ )<sub>n</sub>. Estimation of the CMCs of the  $\text{POS}_n$ -( $\text{C}_{12}\text{TA}$ )<sub>n</sub> with  $n = 1–3$ , assuming ideal mixing of the two-component surfactants and the observed values of the mixed CMC, gives values that are consistent with the nearest related gemini surfactant. However, the POS4 and POS6 systems closely resemble that observed for one class of polyelectrolyte/surfactant mixtures. These observations also support the present conclusion that the gemini-type structure can be fabricated through the electrostatic binding between SDS and BEO.

Herein, taking the existence of the two critical concentrations  $C_1$  and  $C_2$  above, it can be concluded there are at least two aggregate transitions with the variation of the SDS concentration in the system. To understand the transitions, isothermal titration microcalorimetry was also applied. The concentrated SDS/BEO mixed solution with a fixed molar ratio of 5:1 was titrated into water, and the observed enthalpy changes ( $\Delta H_{\text{obs}}$ ) during the titrations are plotted against the final SDS concentration ( $C_{SDS}$ ) in Figure 2c. Beside, both  $C_1$  and  $C_2$  appear in the calorimetric curve, and a more complicated enthalpy change process takes place between these two critical concentrations. Upon the increase of the SDS concentration, the endothermic  $\Delta H_{\text{obs}}$  rapidly decreases, the trend of which is similar to that of SDS micelles being titrated into water. The  $C_1$  value can be identified as the extreme of differentiating observed enthalpy curves with respect to  $C_{SDS}$ . Beyond  $C_1$ , the  $\Delta H_{\text{obs}}$  drops to a minimum point. After the minimum, the  $\Delta H_{\text{obs}}$  gradually increases. Around  $C_2$ , there is an obvious exothermic peak, and finally,  $\Delta H_{\text{obs}}$  gets close to 0. The multiple variations of the  $\Delta H_{\text{obs}}$  curve between  $C_1$  and  $C_2$  imply that additional aggregate transitions exist in this region besides the aggregate transitions at  $C_1$  and  $C_2$ , which are revealed as follows.

To reveal the aggregate transitions in the SDS/BEO mixed solution, DLS and cryo-TEM were used to study the size distribution and morphology of the aggregates at the representative SDS/BEO molar ratio of 5:1, where the samples were chosen in the different SDS concentration stages described above. The DLS and cryo-TEM results are shown

in Figures 3 and 5, and the obtained hydrodynamic radii ( $R_h$ ) of the aggregates from DLS are summarized in Figure 4. When the

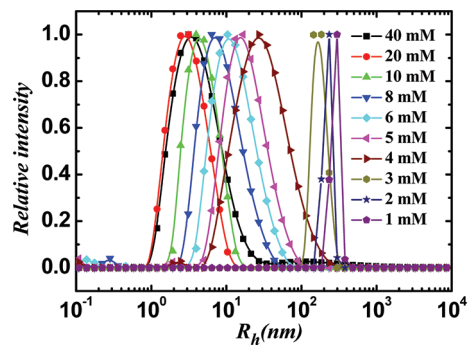


**Figure 3.** The size distribution of the aggregates in the SDS/BEO mixed solution with the molar ratio of 5:1 at different SDS concentrations. The hydrodynamic radius ( $R_h$ ) is plotted with logarithmic scales.

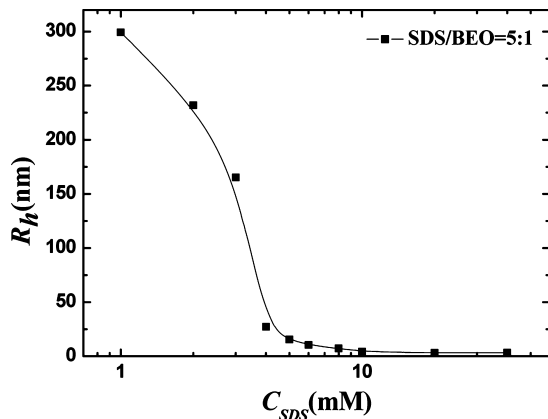


**Figure 4.** The obtained hydrodynamic radii ( $R_h$ ) of the SDS/BEO aggregates with a molar ratio of 5:1 versus the logarithm of the SDS concentration.

SDS concentration is below  $C_1$ , the mixed solution is clear, and the scattering intensity in DLS is too weak to obtain satisfied data. This suggests that the SDS and BEO molecules exist as monomers rather than aggregates in aqueous solution. When the SDS concentration exceeds  $C_1$ , large aggregates generate in the mixed solution. From 1 to 3 mM (between  $C_1$  and  $C_2$ ), the aggregate size from DLS decreases from  $\sim 300$  to  $\sim 160$  nm in radius, and irregular aggregates with diameters above 100 nm are observed in the cryo-TEM images (Figure 5a and b). The irregular aggregates show very light gray color, suggesting that the aggregates should be very loose. From 3 to 4 mM, the aggregate size from DLS starts to sharply drop from  $\sim 160$  to  $\sim 20$  nm in radius. Meanwhile, spherical vesicles with a diameter of  $\sim 50$  nm become the main aggregates, as clearly seen in the cryo-TEM image (Figure 5c). Together with the results in Figure 2,  $C_v$  is designated to be the onset of the transition from irregular aggregates into vesicles. With the further increase of the SDS concentration beyond 4 mM ( $C_2$ ), the average aggregate size from DLS continuously drops to  $\sim 6$  nm. Above 8 mM, the measured aggregate size from DLS is almost invariable with the radius of 3.0–4.0 nm. The cryo-TEM image of the mixed solution at this concentration range presents long thread-like micelles with a diameter of  $\sim 5$  nm and a length

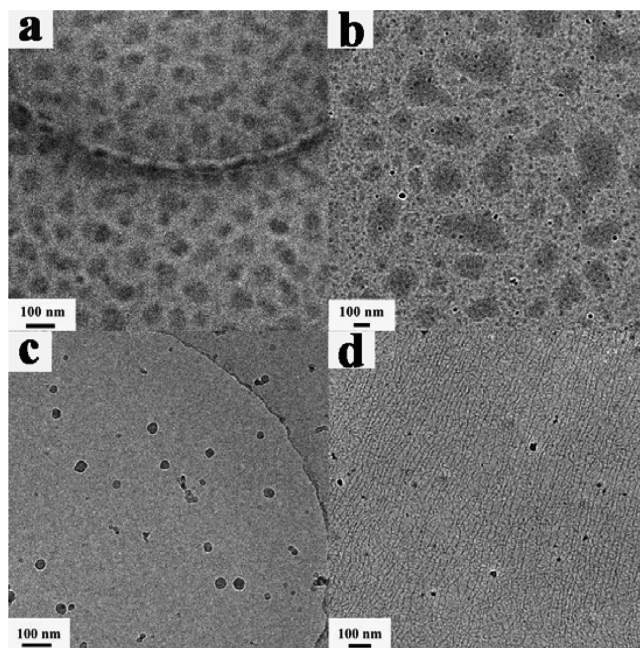


**Figure 5.** Cryo-TEM images of the SDS/BEO mixed solution with the SDS/BEO molar ratio of 5:1 at different SDS concentrations: (a) 1; (b) 2; (c) 4; and (d) 15 mM.

exceeding  $1.5\ \mu\text{m}$  (Figure 5d). Clearly, beyond  $C_2$ , the vesicles are gradually transformed into long thread-like micelles. In brief, with the increase of the SDS concentration, the SDS/BEO mixed solution experiences the following three transitions: the monomers transform into loose large irregular aggregates beyond  $C_1$ , the irregular aggregates transform into vesicles beyond  $C_v$ , and the vesicles finally transform into long thread-like micelles beyond  $C_2$ .

The thermal stability of the SDS/BEO aggregates described above was investigated by a micro-DSC technique. The DSC curves of the SDS/BEO mixed solution with a molar ratio of 5:1 at different SDS concentrations are shown in Figure 6. The solutions at 0.2 and 2 mM SDS (before  $C_2$ ) have not any obvious peaks in the DSC curves in the temperature range studied, while all of the solutions at 4–15 mM SDS (beyond

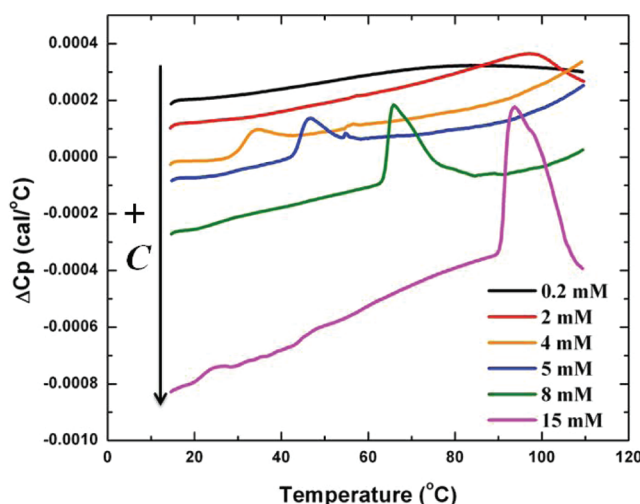


**Figure 6.** Micro-DSC curves of the SDS/BEO mixed solution with the molar ratio of 5:1 at different SDS concentrations.

$C_2$ ) display endothermic peaks. Clearly, both the peak area and the phase transition temperature increase with the increase of the SDS concentration. That is, the thermal stability of the mixed aggregates increases in the order of large irregular aggregates, vesicles and thread-like micelles. This order should be the result of the molecular packing in the aggregates. In general, the stability of aggregates increases with the increase of the compactness of the molecular packing. In addition, it was found that the SDS/BEO mixed solution was clear at low temperature and became turbid at high temperature, which is similar to the property of nonionic surfactants. All of these thermal properties of the mixed solution can be rationalized by the existence of the  $(\text{SDS})_2\text{-BEO}$  gemini structure.

To understand the intermolecular interaction in the aggregate transitions,  $^1\text{H}$  NMR experiments were carried out. Figure 7 shows the chemical shifts in the  $^1\text{H}$  NMR spectra of

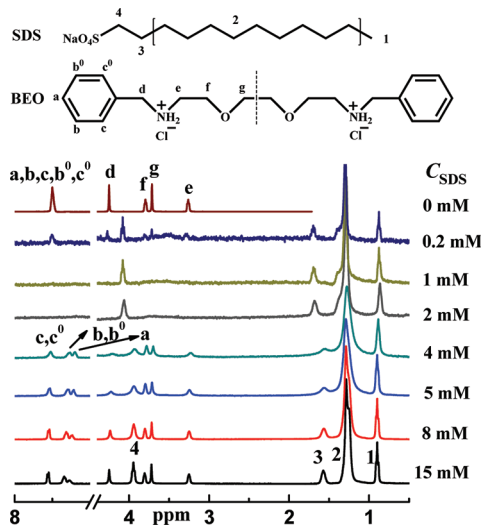


Figure 7.  $^1\text{H}$  NMR spectra of the SDS/BEO mixed solution with the SDS/BEO molar ratio of 5:1 at different SDS concentrations.

the SDS/BEO mixed solution with the molar ratio of 5:1 at the SDS concentrations from 0.2 to 15 mM. The proton signals of the BEO molecules were further distinguished with the aid of 2D NOESY spectrum. The protons of the ammonium groups of BEO have no signals because they are exchanged fast with deuterium. When the SDS concentration is 0.2 mM (before  $C_1$ ), the proton peak of the BEO benzene rings does not show splitting. This means that the BEO and SDS molecules exist as monomers at the low SDS concentration. At SDS concentrations of 1 and 2 mM (beyond  $C_1$ ), the proton signals of the BEO molecules cannot be detected because the large aggregates with a radius much larger than 100 nm limit the sensitivity of the  $^1\text{H}$  NMR technique. Meanwhile, the 3-H and 4-H protons in the SDS hydrocarbon chains have no obvious shifts at this SDS concentration range, which confirms the looser structure of the irregular aggregates just after  $C_1$ . When the SDS concentration reaches 4 mM ( $C_2$ ), the proton peaks of the BEO benzene rings appear again and split into three peaks. According to the integral areas of the peaks, the peak with the highest chemical shift is ascribed to the c-H and  $c^0\text{-H}$  protons, and the sideward peaks correspond to the b-H,  $b^0\text{-H}$ , and a-H protons. Obviously, the a-H, b-H, and  $b^0\text{-H}$  protons are shifted upfield more or less with the addition of SDS, while the c-H and  $c^0\text{-H}$  protons remain almost invariable. Generally, aromatic

protons will shift upfield when they are changed to a less polar environment due to the decrease of the deshielding effect. This means that a-H, b-H, and  $b^0\text{-H}$  protons are located in a relatively nonpolar environment beyond  $C_2$ . The ends of the BEO benzene rings probably insert into the hydrophobic domain of the aggregates. Because of shielding from the BEO benzene rings, the 3-H and 4-H protons of SDS move upfield to a great magnitude. As for the d-H, e-H, f-H, and g-H protons in the spacer, the chemical shifts are almost constant. This demonstrates that the hydrophilic spacer stays in the outer layer of the aggregates.

In summary, the abundant morphologies are generated in the SDS/BEO mixed solution. Figure 8 presents the proposed

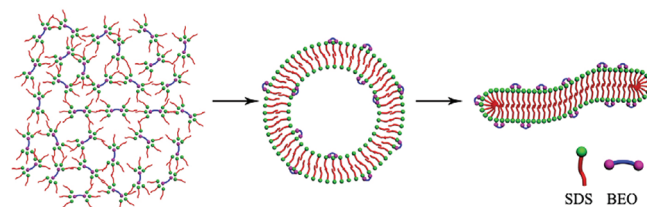


Figure 8. The proposed schematic illustrations of the variation of the aggregate morphologies in the SDS/BEO mixed solution as the total concentration increases.

schematic illustration of the morphology changes in the SDS/BEO mixed solution at the fixed SDS/BEO molar ratio. At the low concentration before  $C_1$ , all of the SDS and BEO molecules exist as monomers because the hydrophobic interaction between the alkyl chains is too weak to allow them to aggregate. When the SDS concentration is beyond  $C_1$ , loose large aggregates with a radius larger than 100 nm are formed. Such an interesting phenomenon should be caused by the special structure of BEO. In the loose large aggregates, one BEO molecule with two cationic charges may bind with two SDS molecules through electrostatic interaction, assisted by the hydrophobic interaction between the hydrocarbon chains of SDS and the benzene rings of BEO. The electrostatic binding leads to the gemini-type structure  $(\text{SDS})_2\text{-BEO}$  as well as the SDS-BEO complex. Thus, the mixed solution may contain three kinds of surfactant structures, the  $(\text{SDS})_2\text{-BEO}$  complexes, the SDS-BEO complexes, and the SDS molecules. Besides, the hydrophobic interactions between the SDS molecules and between BEO and SDS promote all of the surfactant structures to aggregate with each others. Herein, the BEO molecules may play a critical role as bridges to associate the alkyl chains. Thus, the loose network-like irregular aggregates are formed. However, because the hydrophobic interaction is still weak at this stage, ordered and compact aggregate structures cannot be formed. When the SDS concentration exceeds  $C_2$ , the hydrophobic interaction becomes strong enough to transfer the large irregular aggregates into spherical vesicles, where the SDS alkyl chains get close to each others. Beyond  $C_2$ , the SDS molecules turn to be packed more compact due to the progressively increasing hydrophobic interaction of the SDS chains; thus, the vesicles are transformed into long thread-like micelles.

## CONCLUSION

A “gemini-type” cationic organic salt BEO brings rich microstructure transitions in the single-chain surfactant SDS solution. For the SDS/BEO solution, the microstructures of the

aggregates show strong concentration dependence and molar ratio dependence. At a fixed SDS/BEO mixing ratio, upon the increase of the concentration, the SDS/BEO mixtures form large loose irregular aggregates, then spherical vesicles, and finally turn into long thread-like micelles, whose thermal stability increases in the same order. Both the critical aggregation concentration and surface activity of the SDS/BEO solution display the characteristics of gemini surfactants. The SDS/BEO solution can be considered to consist of the  $(\text{SDS})_2\text{-BEO}$  gemini-type complex, the SDS–BEO complex, and excess unbound SDS. This work is helpful to understand the interaction between “gemini-type” organic salts and oppositely charged surfactants. It provides a new approach to construct the surfactant systems with the characteristics of gemini surfactants through intermolecular interaction between a dicationic “gemini-type” organic salt and single-chain surfactant molecules.

## ■ AUTHOR INFORMATION

### Corresponding Author

\*E-mail: yilinwang@iccas.ac.cn.

### Notes

The authors declare no competing financial interest.

## ■ ACKNOWLEDGMENTS

This work was supported by the Chinese Academy of Sciences and National Natural Science Foundation of China (Grants 21025313, 21021003, 20973181, and KJCX1-YW-21-02). We appreciate the State Key Laboratory of Polymer Physics and Chemistry for providing the DLS equipment.

## ■ REFERENCES

- (1) Israelachvili, J. N.; John Mitchell, D.; Ninham, B. W. *J. Chem. Soc., Faraday Trans. 2* **1976**, *72*, 1525–1564.
- (2) Percec, V.; Dulcey, A. E.; Balagurusamy, V. S. K.; Miura, Y.; Smidrkal, J.; Peterca, M.; Nummelin, S.; Edlund, U.; Hudson, S. D.; Heiney, P. A.; et al. *Nature* **2004**, *430*, 764–768.
- (3) Rosen, M. J. *Surfactants and Interfacial Phenomena*, 3rd ed.; Wiley: Chichester, U.K., 2004.
- (4) Menger, F. M.; Littau, C. A. *J. Am. Chem. Soc.* **1991**, *113*, 1451–1452.
- (5) Menger, F. M.; Keiper, J. S. *Angew. Chem., Int. Ed.* **2000**, *39*, 1906–1920.
- (6) Zana, R. *Adv. Colloid Interface Sci.* **2002**, *97*, 203–251.
- (7) Nalluri, S. K. M.; Ravoo, B. J. *Angew. Chem., Int. Ed.* **2010**, *49*, 5371–5374.
- (8) Zhu, B. Y.; Zhao, G. X. *Huaxue Tongbao* **1981**, *6*, 21–26.
- (9) Hu, Z.; Tian, X.; Zhai, Y.; Xu, W.; Zheng, D.; Sun, F. *Protein Cell* **2010**, *1*, 48–58.
- (10) Mysels, K. J. *Langmuir* **1986**, *2*, 423–428.
- (11) Jiang, L. X.; Huang, J. B.; Bahramian, A.; Li, P. X.; Thomas, R. K.; Penfold, J. *Langmuir* **2012**, *28*, 327–338.